Effects of frustration and localization of states in the Penrose lattice

Gerardo G. Naumis and Rafael A. Barrio
Instituto de Física, Universidad Nacional Autónoma de México, Apartado Postal 20-364, 01000 México, Distrito Federal, México

Chumin Wang
Instituto de Investigaciones en Materiales, Universidad Nacional Autónoma de México, Apartado Postal 70-360, 04510, México, Distrito Federal, México

(Received 19 April 1994)

The central gap in the density of states and the localization of states on a Penrose lattice are investigated within a tight-binding model for the vertex problem. The results show that the gap is a consequence of frustration. There are surface states within the gap in a finite lattice. The correlation between the appearance of the gap and the localization of states is also studied.

I. INTRODUCTION

It is well known that the atomic arrangement of solids is essential to determine their physical properties. In fact, the translational symmetry of crystals provides the existence of extended electronic states (Block waves) and disorder induces localization of states.[1]

Since 1984, a new type of structure called quasiperiodic,[2] which is intermediate between periodic and disordered solids, has aroused much interest because new physical properties are expected. Quasicrystals (QC's) are generally metallic alloys with a quasiperiodic structure in three dimensions (3D) [e.g., the I phase in $NiTi_2$ (Ref. 3)] and 2D [e.g., the T phase in $Al_{86}Mn_{14}$ (Ref. 4)]. There are also quasiperiodic systems in 1D, like Fibonacci superlattices which are built with two alternating semiconductors.[5,6] Particularly, the Fibonacci chains provide a simple way to analyze the effects of quasiperiodicity, like the incommensurate folding of the Brillouin zone detected in the Raman spectra of Fibonacci superlattices.[7]

Quasicrystals exhibit an intermediate character between crystals and amorphous; for instance, there is no translational symmetry, like in amorphous materials, but they present sharp diffraction spots like crystals. As for the electronic properties of a QC, we expect intermediate behavior between a crystal and an amorphous solid, for example, in the electronic density of states (DOS) and the localization of states.

In 1D or 2D quasiperiodic systems, three kinds of wave functions coexist: extended, localized, and critical.[8] The critical states are neither localized nor extended; they have self-similar wave functions in real space. For the Fibonacci chain, it has been proved that the spectrum is a Cantor set.[9] However, this chain can only be defined with diagonal (site) or nondiagonal (bond) quasiperiodic sequences, and it does not present another type of topological disorder, like variations in coordination or bond angles, which is an important characteristic in real QC's in more dimensions. One important effect of these topological variations on the electronic properties is the frustration of the wave function, as we shall show later.

The natural extension of the Fibonacci chain in 2D is the Penrose lattice (PL), which is a quasiperiodic way of filling up a 2D planar space with two kinds of tiles. The PL is the lowest-dimensional model with topological quasiperiodicity, and has the advantage of low-dimensional systems which exhibit the effects of disorder more clearly.[10] It would be useful to understand which properties observed in a Fibonacci chain are also valid for a system in higher dimensions.

There are numerous models to study excitations in the PL (Ref. 11) using first principles Hamiltonians. The obvious choices for the atomic positions in these models are the centers (center model[8,10]) and the vertices of the tiles (vertex model[9]). This latter choice is convenient if one is interested in the connectivity properties of the PL and gives insight into the effects of the topology on the excitation spectra. In this paper we shall study the vertex model.

As pointed out by Tsunetsugu *et al.*,[10] the PL would be most sensitive to topological quasiperiodicity, one effect being the frustration induced in the phases of the wave functions. We show here that this frustration and the nonperiodicity are responsible for the central gap in the DOS of the PL.[11] We do this by separating the PL into two alternating sublattices and by renormalizing one of them. This renormalization maps central states into antibonding states. Then, the frustration of the new lattice inhibits antibonding states which means that there is a gap in the DOS of the PL. Also, the nonperiodicity of the lattice produces different amplitudes on each of the sites, which results in a contraction of the band and localization near the lowest band edge.

This paper is organized as follows. In Sec. II we explain the model Hamiltonian and the construction of the tiles for numerical calculations of the DOS. Section III is devoted to the study of the origin of the central gap. Finally, in Sec. IV we give the conclusions of the work.

II. ELECTRONIC PROPERTIES OF THE PENROSE LATTICE

Consider a simple tight-binding Hamiltonian for s electrons, with nearest neighbor interactions

$$H = \sum_{i,j} t_{ij} |i\rangle\langle j|, \tag{1}$$

where sites i and j are vertices of the PL, and the hopping parameter t_{ij} is -1 for connected neighbors and 0 otherwise. In this situation one avoids site or bond disorder. Furthermore, all rings of bonds are fourfold and there is no ring statistics. Therefore only the different coordination of each vertex introduces all the effects of quasiperiodicity.

In order to calculate the DOS one needs to diagonalize a matrix of the order of the number of sites and this represents a severe limitation on the size of the lattice, which is undesirable in a quasicrystal, because the finite size effects cannot be easily identified. We have devised a renormalization method to calculate local DOS in an extremely large Fibonacci chain.[12] Since the PL can be regarded as a straightforward extension of the Fibonacci sequence to 2D, the same method can be extended here.

As the Fibonacci chain is defined by two types of sites, or two types of bonds, the PL can be constructed from two basic tiles. It is convenient to consider the Robinson triangles,[13] obtained when one divides a pentagon. In Fig. 1 these two basic units are shown and can be considered as the tiles of generation 1 and 2, respectively. To obtain the tile of generation 3 one joints the two former tiles $2 \oplus 1$, as shown in the figure. Observe that the second tile to be joined at each step has to be the mirror image of the original one, which is equivalent to follow the matching rules.[14] The shape of a tile of a given generation is always that of one of the two Robinson triangles, and a given shape is repeated every four generations. The ratio of the areas of two tiles of subsequent generations is the golden ratio $\tau = \frac{1}{2}(1+\sqrt{5})$.

The extension of the renormalization procedure followed for the Fibonacci chain[12] is carried out by renormalizing all the interior sites in a given generation, leaving all the sites in the border intact. In terms of the equation of motion for the Green's function $\mathbf{G} = (E\mathbf{I} - \mathbf{H})^{-1}$ this is equivalent to eliminating elements with indexes referring to the interior sites by substituting them into the equations involving only the border sites. As an example consider Fig. 2, in which the tile of generation 5 is shown. Observe that there are only three lengths of bonds $T(1)$, $T(2)$, and $T(3)$, and there is only one interior site labeled 6. The equations of motion are explicitly

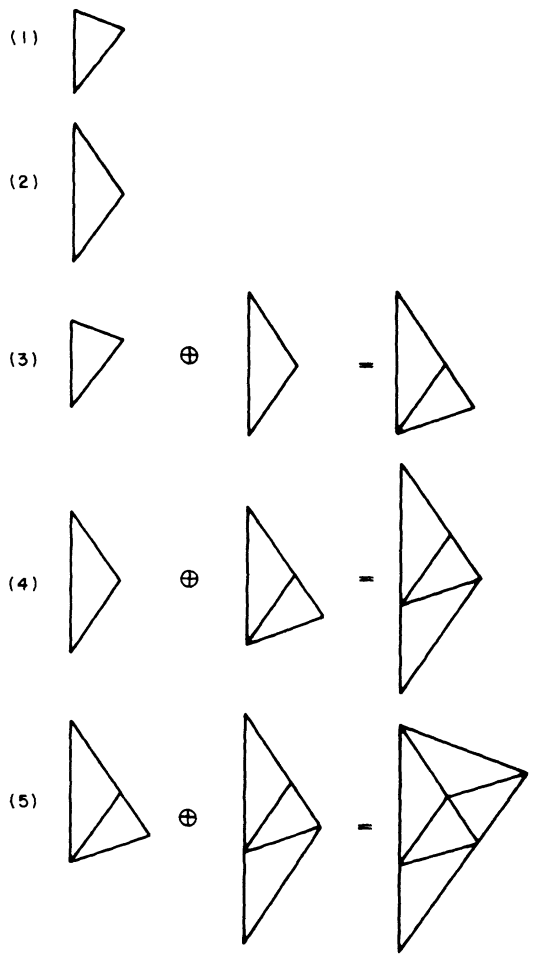

FIG. 1. The two Robinson triangles as Penrose lattices of generations 1 and 2, respectively. Further generations are obtained by joining the previous two.

$$[E - E(1)]\,G(1,1) = 1 + T(2)G(2,1) + T(3)G(5,1),$$
$$[E - E(2)]\,G(2,1) = T(2)G(1,1) + T(3)G(3,1) + T(2)G(5,1) + T(2)G(6,1),$$
$$[E - E(3)]\,G(3,1) = T(3)G(2,1) + T(3)G(4,1) + T(2)G(6,1),$$
$$[E - E(4)]\,G(4,1) = T(3)G(3,1) + T(2)G(5,1) + T(2)G(6,1),$$
$$[E - E(5)]\,G(5,1) = T(3)G(1,1) + T(2)G(2,1) + T(2)G(4,1) + T(1)G(6,1),$$
$$[E - E(6)]\,G(6,1) = T(2)G(2,1) + T(2)G(3,1) + T(2)G(4,1) + T(1)G(5,1).$$

After renormalizing site 6, one is left with only five equations

$$[E - E(1)]\,G(1,1) = 1 + T(2)G(2,1) + T(3)G(5,1),$$
$$[E - E(2) - W22]\,G(2,1) = T(2)G(1,1) + [T(3) + W22]G(3,1) + W22G(4,1) + [T(2) + W12]G(5,1),$$
$$[E - E(3) - W22]\,G(3,1) = [T(3) + W22]G(2,1) + [T(3) + W22]G(4,1) + W12G(5,1),$$
$$[E - E(4) - W22]\,G(4,1) = W22G(2,1) + [T(3) + W22]G(3,1) + [T(2) + W12]G(5,1),$$
$$[E - E(5) - W11]\,G(5,1) = T(3)G(1,1) + [T(2) + W12]G(2,1) + +W12G(3,1) + [T(2) + W12]G(4,1),$$

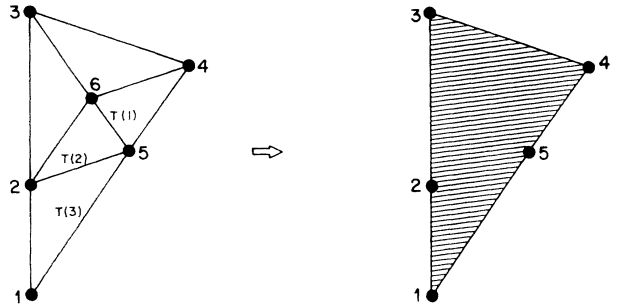

FIG. 2. Penrose lattice of generation 5. There is only one central site labeled 6 and there are three different lengths of bonds. The right-hand side shows the renormalized lattice.

where the effective interactions carry all the information concerning the renormalized site

$$Wij = \frac{T(i)T(j)}{E - E(6)}, \quad i,j = 1,2. \tag{2}$$

The process of tile growing has to be combined with the renormalization at each step. Figure 3 exemplifies this procedure: One renormalizes the interior sites of lattices of generations 7 and 8 leaving only the border sites. Then one joints the two tiles together, and this results in having two new interior atoms for generation 9, which have to be further renormalized. Care has to be taken to include all the renormalized self-energies properly since in further renormalizations the sites include effective bonds and self-energies. Observe that the number of sites to be renormalized in each step grows as the square root of the total number of sites, which grow exponentially with the generation number. This allows to perform calculations in much larger lattices than by direct diagonalization. Notice that the final PL of fat and skinny rhombuses is obtained by setting all the longest $T(3)$ and shortest $T(1)$ bonds to zero.

Figure 4 shows the local DOS at two nearest neighbor sites of a PL of generation 23, containing 14 550 vertices. It can be observed that apart of a complicated structure of bands and gaps, some peculiarities appear. First, the spectra are symmetrical respect to $E = 0$, due to the fact that the lattice is bipartite;[15] i.e., it can be subdivided in two alternating sublattices (say, A and B), and an electron can only hop from an A site onto a B site or back. Then, the Schrödinger equation reduces to $E|j\rangle = -\sum_i |i\rangle$, where if i belongs to A, then j belongs to B or vice versa. Therefore, if E_n is an eigenvalue, $-E_n$ is always an eigenvalue too, because their eigenfunctions differ only on the sign of the wave function of one sublattice.

Likewise, one observes in Fig. 4 three main features:

(1) The bandwidth is larger than $2\langle Z\rangle$, where the mean coordination number is $\langle Z\rangle = 4$ in the PL.

(2) A highly degenerate state at $E = 0$.

(3) A gap separating the states at $E = 0$ from the rest.

The two first features have been carefully studied. For the bandwidth there are estimations based on a finite size scaling[15] and a mean field approach.[16] In the latter it is supposed that all the amplitudes for each local configuration that appears in the PL are the same. In both cases the maximum eigenvalue is $E = 4.23$, which is very close to the numerical result. Concerning the central peak $E = 0$, it consists of fractally confined states,[15] which are strictly confined in fractally distributed regions.

Finally, the persistence of the gap around $E = 0$ in an infinite PL is not clear yet. We have verified that the gap width (Δ) does not diminish beyond ≈ 0.15 even for the largest lattices ($\approx 10^4$ atoms). We noticed a cycle of Δ with a four-generation period, which is certainly due to the construction period of the lattice.[16] It is worth mentioning that the method of renormalization allows one to calculate the local DOS in any chosen site, and that the features shown in Fig. 4 are present no matter which site is chosen. We also calculated the integrated DOS and the total DOS and we checked that the gap is also present there.

To examine the localization of electronic states in the PL we calculate the inverse participation ratio (IPR). If the eigenfunction of state E_j is $\psi_j = \sum_i C_i(j)|i\rangle$, then the IPR for the eigenstate j is defined as

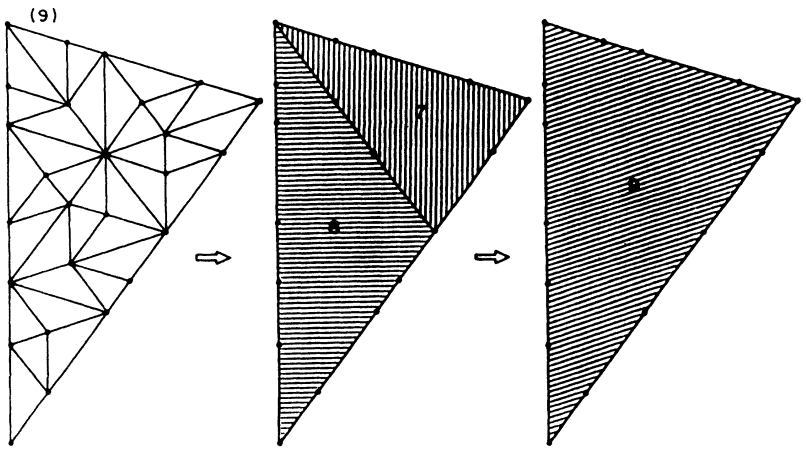

FIG. 3. A sketch representing the renormalizarion of the central sites of lattices 7 and 8. The final lattice of generation 9 is obtained by renormalizing the border sites between the former two in the equations for the Green's functions.

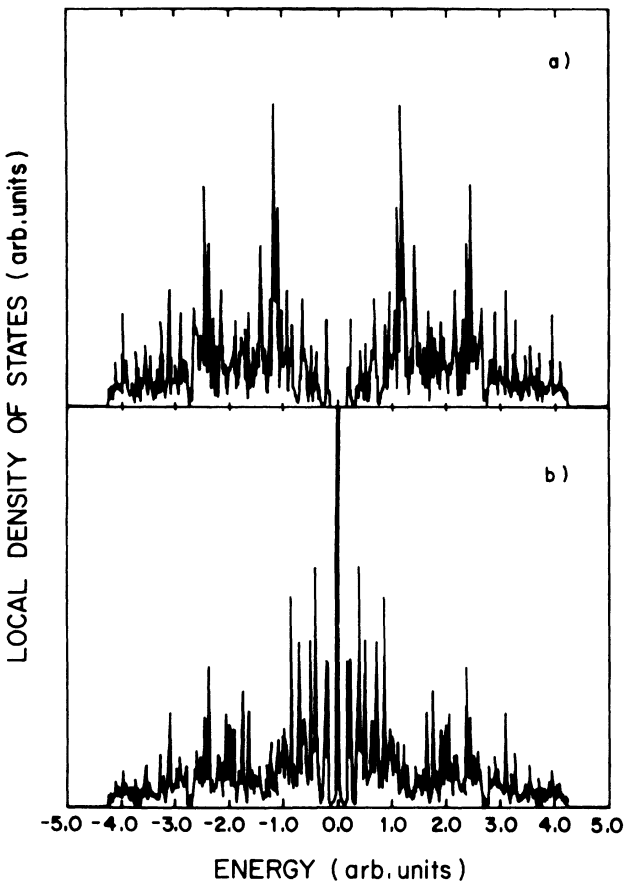

FIG. 4. Local density of states from a Penrose lattice of generation 23. (a) is taken from a three-coordinated site and (b) from a contiguous four-coordinated site.

$$\mathrm{IPR}(j) = \sum_{i=1}^{N} C_i(j)^4. \tag{3}$$

The IPR is a measure of the reciprocal of the number of sites occupied by the wave function.[8] In Fig. 5 the IPR as a function of the energy for a lattice of $N = 2176$ sites is shown. Surface states are detected in the IPR by performing several calculations in clusters of different sizes and different boundary conditions.

The IPR values are between 0.06 and $1/N$ for all the studied Penrose lattices. We can see in Fig. 5 that states near the edges of the band are delocalized with an IPR closer to $1/N$. The vertical line of dots at $E = 0$ corresponds to confined states, since their IPR presents a minimum value (dashed line in Fig. 5), which corresponds to the maximum extension of the fractal regions.

States at $|E| \leq 0.15$ (with arrows in Fig. 5) are exponentially localized because their IPR does not vary with N. They also have the highest IPR. These states only present amplitude different from zero near the surface, since Conway's theorem[15] would imply that if there is a configuration of sites with a given amplitude, there should be a similar configuration at a distance not exceeding twice the radius of the configuration. Therefore, they are certainly surface states, not present in the infinite lattice.

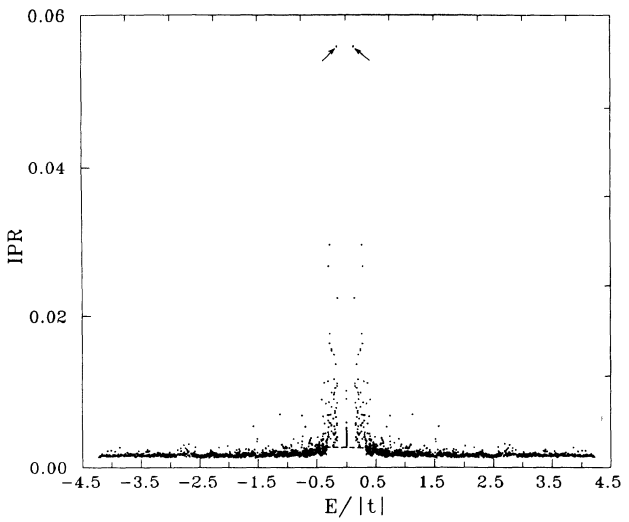

FIG. 5. Inverse participation ratio (IPR) for a Penrose lattice of generation 19 obtained by exact diagonalization. The lowest level corresponds to states with $C_i(j)$ close to $1/\sqrt{N}$. The dashed line indicates the lowest IPR of the degenerate central states, and some surface states with constant IPR are indicated by arrows.

Figure 5 shows that for energies below ≈ 0.37, the behavior of the IPR changes. All states with an absolute energy below this value have an IPR bigger than the lower IPR value of the central state (dashed line in the figure). This figure shows that states below 0.37 are not extended. We shall discuss their nature in the next section.

More information can be extracted if one plots the quantity "site amplitude contribution" (SAC), defined as

$$\mathrm{SAC}(\nu, j) = \frac{1}{N_\nu} \sum_{i \in \nu}^{N_\nu} C_i(j)^4, \tag{4}$$

for all sites with coordination ν excluding those in the surface. In Fig. 6 this quantity is shown for sites of co-

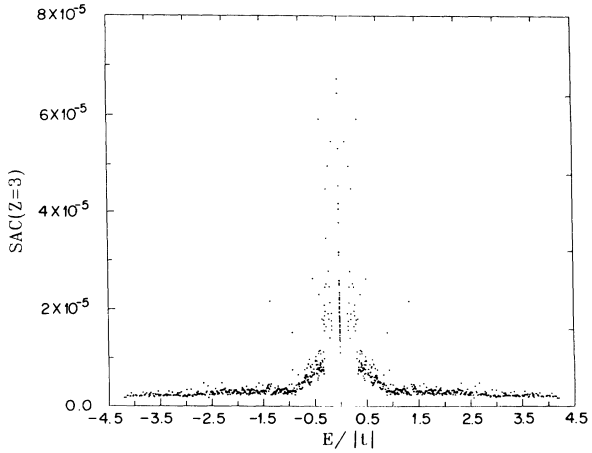

FIG. 6. Site amplitude contribution (SAC) for all sites of coordination 3 in a Penrose lattice of generation 17. Notice the abrupt change of behavior around $E = 0.92$ and the sudden increase at $E = 0.37$.

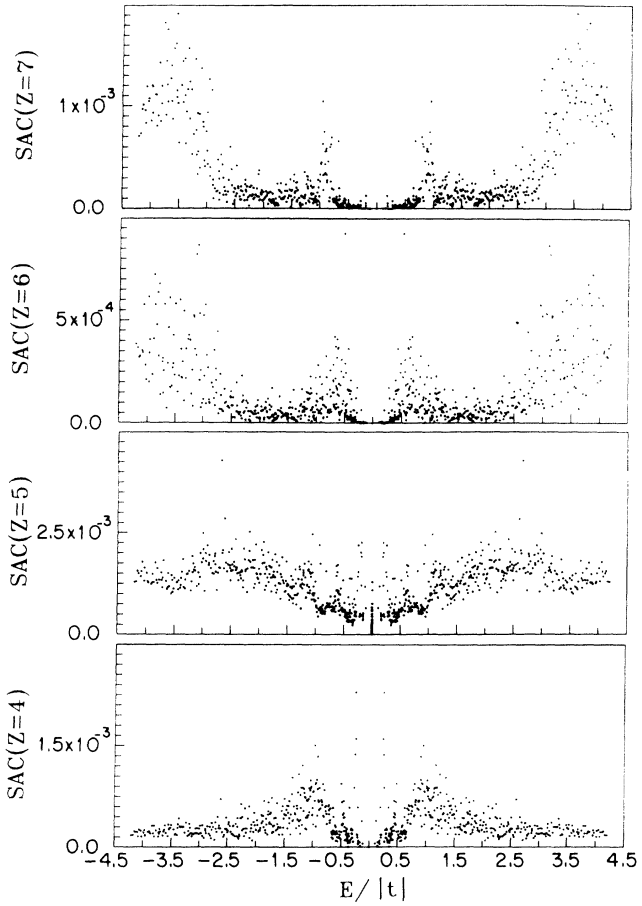

FIG. 7. The same as in Fig. 6 for sites of other coordinations, indicated in each plot. The value of the gap at $E = 0.2$, and the other peculiar values $E = 0.37$ and $E = 0.92$ are also noticeable here.

ordination 3. Notice that a higher value of this quantity means a larger amplitude in three-coordinated sites of the corresponding eigenfunction. It is seen that the behavior of this plot changes at $E \approx 0.92$ and at $E \approx 0.37$. This latter value corresponds to the localization edge detected in Fig. 5, and the value 0.92 is peculiar because here the eigenstates with $|E| \geq 0.92$ have constant amplitude in three-coordinated sites.

In Fig. 7 the corresponding plots for all the other coordinations are shown. Notice that the states near the center of the spectrum present more amplitude in sites of lower coordination, while the higher coordination sites have amplitude near the band edges. This is in agreement with the fact that there is not crossing of the bands when one varies the ratio between the hopping parameter and the site energy.[17] It also supports the statement of level repulsion (quantum chaos) in other quasiperiodic 2D systems.[18]

III. FRUSTRATION IN H^2

Since the PL is bipartite, in this section we renormalize one of the original sublattices and define the corresponding Hamiltonian ($H^2\Psi = E^2\Psi$). Then we study the consequences of frustration and nonperiodicity in the renormalized lattice.

After renormalizing one of the sublattices the corresponding Hamiltonian is

$$H^2 = t^2 \sum_{i \in A} \left[Z_i |i\rangle\langle i| + 2 \sum_{l}^{Z_i} |i\rangle\langle l| + \sum_{k}^{M_i} i\rangle\langle k| \right] . \quad (5)$$

Sites l and k are the second nearest neighbors of i in the original lattice. If i is situated in a corner of a rhombus, l is one of the Z_i sites on the opposite corner of that rhombus. k is one of the $M_i = \sum_j (Z_j - 3)$ second neighbors of i that belongs to a rhombus that does not have i as a corner. Here j is a first neighbor of both i and k.

After renormalization, the new lattice (which we shall call $H2$) is composed by two kinds of regions. One with only triangular cells (regions I) centered in renormalized three-coordinated sites, which do not present crossed (second neighbor like) interactions. The other type presents crossed interactions (k bonds) and is composed by cells, of six different shapes, defined by l bonds (regions II in Fig. 8). These cells represent the dual of renormalized vertices with coordination other than 3.

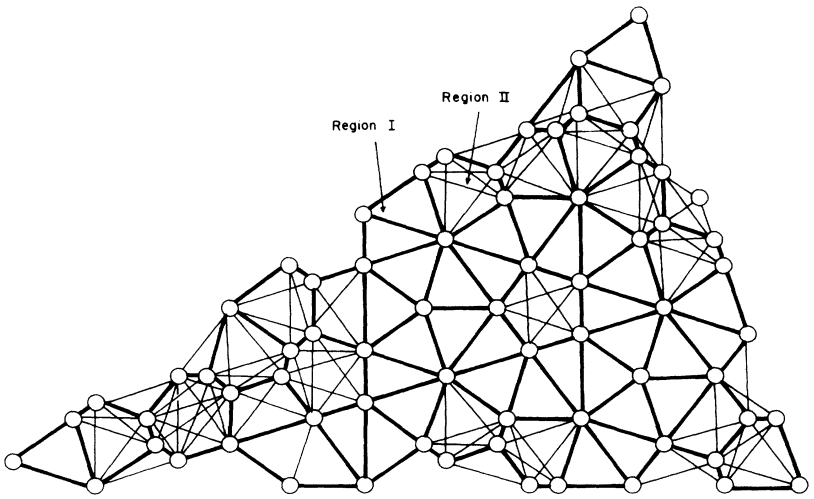

FIG. 8. Sketch of a portion of a $H2$ lattice obtained after renormalizing one of the alternating sublattices of the PL. Region I only contains triangular cells and region II presents second-neighbor-like interactions due to k bonds (in light lines) and first neighbor interactions due to l bonds (in bold lines).

This division is due to the fact that in the PL all non-three vertices are connected in lines (called strings) which divide the whole lattice in finite independent parts.[19] These parts contain only three-edge vertices. The same strings confine inside them all eigenstates at $E = 0$ (the amplitude of the wave function is always zero in the strings).[15,19] As was found by Khomoto and Sutherland[15] almost all non-three-edge vertices are sites with zero amplitude at $E = 0$, which means that almost all sites in a region I have zero amplitude too.

The effect of the renormalization is immediately seen when one realizes that the center of the band in the original Hamiltonian is mapped to the minimum eigenvalue of H^2. Since in H^2 the hopping parameter (t^2) is positive, then its highest eigenvalue corresponds to the bonding state while the minimum eigenvalue ($E^2 = 0$) corresponds to an antibonding state in which the amplitude of neighbor sites changes sign (maximum number of nodes).

The bonding limit is always realizable for all structures.[20] The situation is quite different for the totally coherent antibonding state. In a structure with odd-membered rings this is not possible because there are frustrated bonds, i.e., bonds which connect sites with the same phase. Thus, a completely antibonding state is not realizable. The closest one can get to the antibonding state is to arrange the coefficients $C_i(j)$ of the wave function as to minimize the number of frustrated bonds.[21] Moreover, states near this antibonding state can be expected to be profoundly affected by topological disorder.[21] In the renormalized PL one expects a gap, due to frustration, between the lowest eigenvalue ($E^2 = 0$, which is confined) and the first band state. It is also expected a change in the localization properties of states near the antibonding edge.

The edge due to frustration corresponds to a state with the minimum number of frustrated bonds (see the Appendix). As a first approximation let us calculate this edge by assuming that all cells in $H2$ have the minimum number of frustrated bonds, and that there are no variations of the amplitudes C_i. Locally, there are eight types of cells μ in the $H2$ lattice (using the usual notation[14] for μ; see Table I), or if one considers cells with the same number Z_μ of sides as equivalent, there are only five types. Note that the number of sides is exactly the coordination of the renormalized site in the PL at the center of the cell. Adapting the expressions derived in the Appendix, the frustration edge, given by Eq. (A7), can be written as

$$E_f^2 = t^2\left[\sum_\mu Z_\mu P_\mu - 2\sum_\mu P(\mu)N_t(\mu) + 4\sum_\mu P(\mu)N_f(\mu)\right]. \quad (6)$$

Here the summations are over *cells*; therefore $P(\mu)$ is the proportion of type μ vertices in the PL, which is also the relative number of the corresponding dual cells in $H2$. Observe that $C_i = \sqrt{2/N}$ in $H2$ and

TABLE I. Types of cells in $H2$.

Phase • = +1 ∘ = −1	Cell Name (μ)	Z_μ	$P(\mu)$
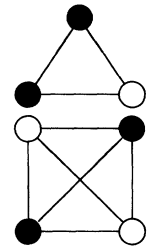	Q, D	3	7-4τ
	K	4	5τ-8
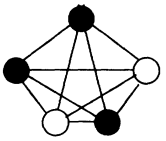	S, S_5, J	5	10-6τ
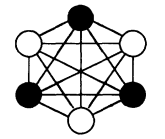	S_4	6	13τ-21
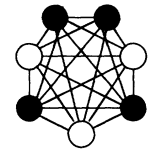	S_3	7	13-8τ

$$\sum_{i\in A}^{N/2} Z_i C_i^2 = \sum_{\mu\in PL}^{N} P(\mu)Z_\mu = \langle Z\rangle = 4.$$

The second term in the right-hand side of Eq. (6) is obtained by counting the total number of bonds $N_t(\mu)$ in each type of cell. Bonds of type k in Eq. (5) belong to only one cell, while bonds of type l share two cells; see Fig. 8. Therefore, the latter should have a weight of 1/2, which cancels the factor of 2 in the hopping parameter of bonds l. Thus, when counting bonds in a cell all bonds have the same weight. In the third term only the number of frustrated bonds per cell $N_f(\mu)$ contribute with $f(m,n) = 4$, if one does not allow the relative phase between sites m and n, connected by a frustrated bond, to deviate from zero.

Inspection of Table I shows that $N_t(\mu) = Z_\mu(Z_\mu - 1)/2$ and that

$$N_f(\mu) = \begin{cases} Z_\mu(Z_\mu - 2)/4 & \text{if } Z_\mu \text{ is even,} \\ (Z_\mu - 1)^2/4 & \text{if } Z_\mu \text{ is odd.} \end{cases}$$

Notice that these numbers are not altered if one makes another choice of the phases, provided that one conserves the number of positive and negative signs. By putting those values in (6) we get

$$E_f^2 = \sum_\mu P(\mu)\,[Z_\mu - 2\,\{N_t(\mu) - 2N_f(\mu)\}] = \sum_{\mu\ \text{odd}} P(\mu). \tag{7}$$

In our case the numerical result, obtained from Table I is

$$E_f^2 = P(Q) + P(D) + P(S) + P(S_5) + P(J) + P(S_3) = \frac{6}{\tau^4} = 0.8754$$

or $E_f = 0.9356$. This number corresponds to the value in Fig. 6 where the wave functions start having amplitude preferentially in sites with $Z = 3$. Therefore, based on the ideas in the Appendix let us assume that states below E_f^2 in $H2$ present amplitude concentrated at the vertices of cells other than $Z_\mu = 3$ (regions II) in order to reduce frustration.

Let us calculate a minimum bound to these states by assuming that the amplitude at all vertices other than 3 is zero. That is, there is no contribution to the wave function from any triangular cell in this minimal state. All cells become even except cells of type S, two J for each S_4 site, and all the S_4, which become triangles. Therefore, the new lower limit for states with varying amplitude is

$$E_l^2 = P(S) + 3P(S_4) = \frac{184\tau - 297}{5} = 0.1436$$

or $E_l = 0.3790$, which is very close to the calculated value in Fig. 6 and the value $0.37 < E_l < 0.55$ obtained by the method of continued fractions.[22]

States between E_l and E_f are mainly localized in regions II and they are not fully extended. Examination of the wave functions of states below E_l suggests that they are fractally localized, in the sense that states close to E_l concentrate the amplitude inside the surroundings of the fivefold symmetry center (S or S_5) of the largest inflated PL. As the energy is lower, the amplitude peaks around the fivefold centers of PL with smaller rhombuses. Therefore, it is reasonable to say that the lower energy limit for this kind of state is when the amplitude concentrates around all the fivefold sites. An estimate for this limit will give the gap

$$\Delta^2 = P(S) + P(S_5) = \frac{1}{\tau^6} = 0.0557 \tag{8}$$

or $\Delta = 0.236$, in close agreement with the narrow band found by Kumar *et al.*[22] and in our numerical calculation. One should notice that an inflated PL with all the vertices in S or S_5 has rhombuses with sides of length τ^3, which means that one has a characteristic minimum distance to fractally deflate the states around the fivefold symmetry centers. This fractallity has been observed in PL built with piezoelectrics with a vibrating oil membrane.[23] In these experiments, when the wavelength was comparable to the distance between vertices, or smaller, features at typical distances showing the deflation rules of the PL were observed; that is, the amplitude of oscillation is greater where there should be a fivefold symmetry center inside the rhombuses. As the smallest strings are formed around a S_5 site (S_0 string in Ref. 19) one is tempted to say that the value of the gap should be $\Delta = \sqrt{(3-\tau)/5}/\tau^3 = 0.1241$ according to Eq. (8). However, more numerical calculations are required to verify this speculation.

As a token, Eq. (6) can be used to estimate the bonding edge E_b, noticing that in the bonding limit all bonds are frustrated. Then $N_f(\mu) = N_t(\mu)$, which gives

$$E_b^2 = \sum_\mu P(\mu) Z_\mu^2 = 3Z_\mu + 2N_k(\mu) = 66 - 30\tau = 17.458\,98$$

or, in the PL, $E_b = 4.1784$. The difference with respect to the observed value ($E_b = 4.23$) is due to variations of the amplitudes in each kind of vertex, not taken into account here. If one allows changes in the amplitude, one reproduces the mean field result,[12] which is correct. Note that in a square lattice (SQL) $E_b = 4.00$. This difference arises from the fact that in the renormalized SQL the numbers of bonds l and k are $2N$, but in the renormalized PL the number of bonds l is $2N$ while the number of k bonds is $N_k = (27 - 15\tau)N = 2.729N$. Another way of saying it is that the widening of the band is a consequence of the coordination fluctuations or the second moment of Z.

The method presented here can be applied to the *center model*,[10] in which there is contraction of the upper limit of the band of about 1.32. This is due to frustration in the PL formed with sites of coordination 4, but rings of different shapes, as in $H2$. Assuming again that there are no amplitude variations, this contraction should be given by Eq. (A11) $E_\Delta = 4N_f/N = 2[1 - P(K) - P(S_4)] = 1.75$, which is larger than the observed value in the DOS, but very close to the place in which the IPR changes from being constant.[8]

IV. CONCLUSIONS

In this paper a detailed examination of the tight-binding spectrum of the vertex model in a PL was presented. Numerical calculations, made in large PL's built with a renormalization procedure, suggest the persistence of the central gap in an infinite PL. A theory based on frustration ideas in a renormalized lattice ($H2$) was presented, and some peculiar values of the energy were singled out by the theory. At $E = 0.9356$ the theory predicts a change of the nature of states, progressively delocalized above it and localized in specific regions to reduce frustration below it due to amplitude variations. At $E = 0.3790$ a lower limit for these localized states in regions of low frustration is found, and as one lowers the energy the states are fractally localized around points of fivefold symmetry. We also found that $E = 0.236$ represents an estimation for the lower limit for these fractally localized states, and therefore an estimation of the gap. The numerical calculations in finite PL agree extremely well with these values of the energy, except that some states below 0.2 are found in the calculations. Some of

these states are evidently due to finite size effects, and are confined to the surface of the lattice. However, some states between $E = 0.154$ and 0.23 conserve some of the fractal properties around fivefold centers. More theoretical investigation is required to fully understand the states between 0.15 and 0.37. This work is currently in progress. The theory can be applied to other quasiperiodic lattices as the PL central model or octagonal quasicrystals.

ACKNOWLEDGMENTS

We are thankful to R. B. Stinchcombe, D. Sherrington, and D. Weaire for useful comments. We acknowledge M.F. Thorpe for pointing out to us the properties of $H2$. This work was supported in part by DGAPA-UNAM under Grant No. IN-103493, and by the Commission of the European Communities through Contract No. CI1-CT90-0864 (DSCN).

APPENDIX: ESTIMATION OF THE BAND EDGE

Our aim is to find an expression for the band edge of an antibonding state. Suppose that we have the following tight-binding Hamiltonian:

$$H = \sum_i \left(Z_i |i\rangle\langle i| + \sum_j V_{ij} |i\rangle\langle j| \right); \tag{A1}$$

then we construct a wave function with minimal frustration,

$$|M\rangle = \sum_i C_i e^{i\theta_i} |i\rangle. \tag{A2}$$

This wave function is not necessarily an eigenstate of Eq. (A1) but the expectation value of the energy calculated using this function can serve as an approximation of the band edge. Using Eq. (A1) we obtain the expression

$$E_0 = \langle M|H|M\rangle = \sum_i \left(Z_i \langle M|i\rangle\langle i|M\rangle + \sum_j V_{ij} \langle M|i\rangle\langle j|M\rangle \right). \tag{A3}$$

The term $\langle M|i\rangle\langle i|M\rangle$ always gives C_i^2. If the bond between i and j is not frustrated, then $\langle M|i\rangle\langle j|M\rangle = -C_i C_j$. Otherwise, we label sites connected by the frustrated bond by m and n, and

$$\langle M|i\rangle\langle j|M\rangle = C_m C_n e^{i(\theta_m - \theta_n)}. \tag{A4}$$

Then,

$$E_0 = \sum_i \left[Z_i C_i^2 - \sum_j{}' V_{ij} C_i C_j \right] + \sum_{m,n} V_{mn} e^{i(\theta_m - \theta_n)} C_m C_n. \tag{A5}$$

The primed summation is carried out over nonfrustrated vertices. We rewrite this expression as

$$E_0 = \sum_i \left[Z_i C_i^2 - \sum_j V_{i,j} C_i C_j \right] + \sum_{m,n} V_{mn} [\exp i(\theta_m - \theta_n) + 1] C_m C_n. \tag{A6}$$

In this equation, the sum over j is now over all the neighbors of site i. If the last sum is made over frustrated bonds, instead of sites, we get

$$E_0 = \sum_i \left[Z_i C_i^2 - \sum_j V_{ij} C_i C_j \right] + \sum_{f \text{ bonds}} 2V_{mn} [\cos(\theta_m - \theta_n) + 1] C_m C_n. \tag{A7}$$

We can see that there are two contributions to the displacement of the band edge,

$$\Delta_A = \sum_i \left[Z_i C_i^2 - \sum_j V_{ij} C_i C_j \right] \tag{A8}$$

and

$$\Delta_F = \sum_{f \text{ bonds}} V_{mn} f(m,n) C_m C_n, \tag{A9}$$

with

$$f(m,n) = 2[\cos(\theta_m - \theta_n) + 1]. \tag{A10}$$

One is due to the different amplitudes in each site (Δ_A). For a crystal this term is zero since Z_i is a constant and all the amplitudes are the same, but for nonperiodic lattices this term may not be zero. The other contribution (Δ_F), is produced by the frustration of the lattice and can be reached either by changing the phase or the amplitudes on sites connected by frustrated bonds. Note that in a periodic lattice this term could be different from zero. For perfectly frustrated bonds in a lattice with constant Z and $V_{ij} = V$ for nearest neighbors we have that $f(m,n) = 4$, and

$$E_B = 4VN_f/N, \tag{A11}$$

where N_f is the minimum number of frustrated bonds

As an example, the compression of the DOS due to frustration in a triangular lattice can be calculated. In this case the coordination is 6, and we expect that the DOS limits are 0 and 12 for the Hamiltonian (A1). However, the basic cell of this lattice is a triangle, and we cannot construct an antibonding state. Then, we need to use a trial function with minimal frustration to calculate the lower band edge. The symmetry of the lattice suggest that the greatest difference of phases between sites is $\pi/3$ with constant amplitude. Then, using Eq. (A10) it is found that $f(m,n) = 1$ and $\Delta_A = 0$. Note that all sites are joined by frustrated bonds. By applying Eq. (A9), we find that the lower limit of the band is

$$E_0 = \sum_{f \text{ bonds}} C_m C_n = 3. \tag{A12}$$

The last step follows from the fact that the number of frustrated bonds is equal to the total number of bonds, in this case $3N$. All the amplitudes are $1/\sqrt{N}$. The example of triangular cells is the only one in which frustration is reduced by distributing the phase uniformly among the sites in the ring. In cells with a larger odd number of sites a variation of the phases does not leed to a smaller frustration with respect to the state in which the phases differences are π in most consecutive sites.

[1] E.N. Economou, *Green's Functions in Quantum Physics*, 2nd ed., Springer Series in Solid State Sciences, Vol. 17 (Springer, New York, 1983).

[2] D. Schechtman, I. Blech, D. Gratías, and J.W. Cahn, Phys. Rev. Lett. **53**, 1951 (1984).

[3] T. Janssen, Phys. Rep. **168**, 55 (1988).

[4] J. Reyes, J.G. Pérez-Ramírez, and R. Pérez, J. Mater. Res. **3**, 29 (1988).

[5] R. Merlin, K. Bajema, R. Clarke, F.Y. Juang, and P.K. Bhattacharga, Phys. Rev. Lett. **55**, 1768 (1985).

[6] M.W.C. Dharma-Wardana, A.H. MacDonald, D.J. Lockwood, J.M. Baribeau, and D.C. Houghton, Phys. Rev. Lett. **58**, 1761 (1987).

[7] C. Wang and R. Barrio, Phys. Rev. Lett. **61**, 191 (1988).

[8] P. Ma and Y. Liu, Phys. Rev. B **39**, 9904 (1989).

[9] M. Kohmoto, B. Sutherland, and C. Tang, Phys. Rev. B **35**, 1020 (1987).

[10] H. Tsunetsugsu, T. Fujiwara, K. Ueda, and T. Tokihiro, Phys. Rev. B **43**, 8879 (1991).

[11] J.M. Cabrera-Trujillo, F. Mejia-Lira, and J.L. Moran-Lopez, in *Proceedings of the 2nd. Latin American Workshop on Non- Linear Phenomena*, edited by P. Cordero and R. Benguria (Elsevier, New York, 1991).

[12] R.A. Barrio and Chumin Wang, in *Quasicrystals and Incommensurate Structures in Condensed Matter*, edited by M. José Yacamán, D. Romeu, V. Castaño, and A. Gómez (World Scientific, Singapore, 1990), p. 448.

[13] R. Robinson, Invent. Math. **12**, 177 (1971).

[14] N.G. de Bruijn, Proc. K. Ned. Akad. Wet. A **84**, 53 (1981).

[15] M. Kohmoto and B. Sutherland, Phys. Rev. Lett. **56**, 2740 (1986).

[16] R.A. Barrio and C. Wang, J. Non-Cryst. Solids **153&154**, 375 (1993).

[17] M. Kohmoto and B. Sutherland, Phys. Rev. B **34**, 3849 (1986).

[18] V.G. Benza and C. Sire, Phys. Rev. B **44**, 10343 (1991).

[19] M. Arai, T. Tokihiro, T. Fujiwara, and M. Khomoto, Phys. Rev. B **38**, 1621 (1988).

[20] M.H. Cohen, in *Topological Disorder in Condensed Matter*, edited by F. Yonezawa and T. Ninomiya, Springer Series in Solid State Sciences, Vol. 46 (Springer, New York, 1983), p. 122.

[21] M.H. Cohen, in *Fundamental Physics of Amorphous Semiconductors*, edited by F. Yonezawa, Springer Series in Solid State Sciences, Vol. 25 (Springer, New York, 1981), p. 119.

[22] V. Kumar, D. Sahoo, and G. Athithan, Phys. Rev. B **34**, 6924 (1986).

[23] F. Montero de Espinosa and M. Torres, Appl. Phys. Lett. (to be published).